Environment-Aware Estimation of Battery State-of-Charge for Mobile Devices

Liang He
University of Colorado–Denver, CO
liang.he@ucdenver.edu

Youngmoon Lee, Eugene Kim, Kang G. Shin
University of Michigan–Ann Arbor, MI
{ymoonlee,kimsun,kgshin}@umich.edu

ABSTRACT

Reliable operation of mobile devices, such as smartphones and tablets, has become essential for great many users around the globe. Mobile devices, however, have been reported to suffer from frequent, unexpected shutoffs — e.g., shutting off even when their batteries were shown to have up to 60% remaining state-of-charge (SoC) — especially in cold environments. Their main cause is found to be the inability of commodity mobile devices to account for the strong dependency between battery SoC and the environment temperature. To remedy this problem, we design, implement, and evaluate `EA-SoC`, a real-time Environment-Aware battery SoC estimation service for mobile devices. `EA-SoC` estimates the battery SoC by predicting the end-of-discharge battery resistance, grounding on (1) a thermal circuit model that describes the interactions among the battery's discharge current, temperature, and the environment, and (2) an empirically validated data-driven model on the relations between battery temperature and resistance. We have conducted 35 experimental case-studies with two Nexus 5X smartphones to evaluate `EA-SoC`. `EA-SoC` is shown to report an average of 3% SoC when the phones shut off even in a -15^oC environment, while that reported by the phones' built-in fuel-gauge chips could be over 90%.

ACM Reference format:
Liang He and Youngmoon Lee, Eugene Kim, Kang G. Shin. 2019. Environment-Aware Estimation of Battery State-of-Charge for Mobile Devices. In *Proceedings of ACM Conference, Montreal, Canada, April 2019 (ICCPS'19),* 10 pages.
DOI: 10.1145/nnnnnnn.nnnnnnn

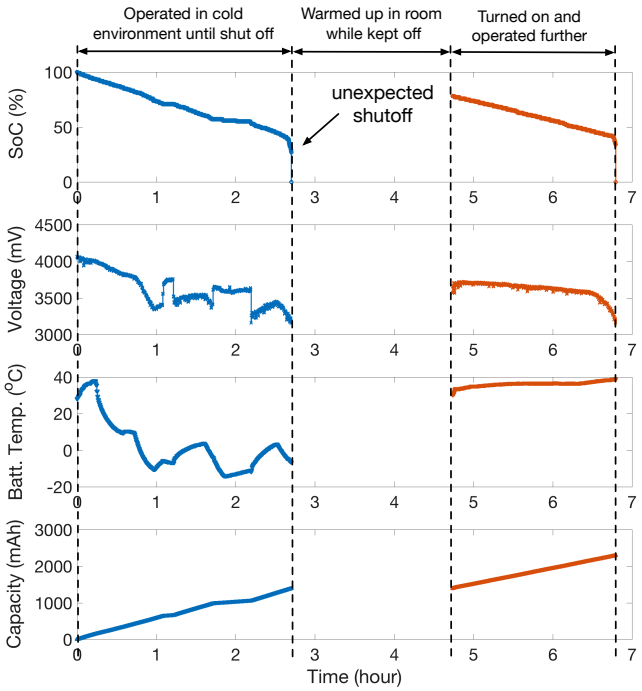

Figure 1: Unexpected shutoff of Xperia Z smartphone in a cold environment: the phone operates in a -15^oC environment and shuts off even when it was shown to still has 30% SoC, which is then turned back on and operated for about 2 more hours after warming up to room temperature.

1 INTRODUCTION

Mobile devices have become essential to great many people, and their reliable operation depends strongly on the timely and accurate estimation of their battery state-of-charge (SoC). Mobile users, however, have frequently complained about the unexpected shutoffs of their devices due to inaccurate/untimely SoC estimation [2, 4, 5] — i.e., the devices were shut off even when their remaining power was shown to be up to 60% of full power [8], especially in a cold environment [6]. Fig. 1 illustrates such an unexpected shutoff of Xperia Z smartphone:[1] (i) video streaming in a -15^oC environment, the phone shut off prematurely when it was shown to have 30% state-of-charge (SoC); (ii) the phone, after shutting off, was moved to and kept in a room-temperature environment for 2 hours; (iii) the phone, without charging it, was turned back on again and operated for about 2 more hours.

These premature shutoffs of mobile devices are due to the failure of their fuel-gauge chips to capture the environment-dependent battery performance, thus leading to erroneous estimation of their real-time SoCs. Cold temperature increases the internal resistance of batteries, thus degrading batteries' ability to deliver both the stored energy (i.e., the energy that can be delivered to operate the devices) and power (i.e., the maximum discharge power the battery can supply) [13, 15, 25, 30, 32]. When moving a mobile device from a warm to a cold environment, the fuel-gauge chip of the device

ICCPS'19, Montreal, Canada

DOI: 10.1145/nnnnnnn.nnnnnnn

[1] We conducted similar experiments with Nexus 5X and Nexus 6P smartphones and made similar observations.

cannot sense the change of the environment and thus cannot accurately predict the battery's end-of-discharge condition. This, in turn, leads to the over-estimation of battery's remaining power supply, i.e., SoC, and thus unexpected shutoffs. Note that unexpected shutoffs also risk deep-discharging and accelerate battery degradation [22, 31].

To address this problem, we design and implement EA-SoC, an environment-aware battery SoC estimation service for mobile devices that achieves accurate SoC estimation even in a cold environment. EA-SoC compensates the environment's impact on battery SoC by predicting the battery's end-of-discharge temperature in real time, and then estimating the end-of-discharge battery resistance according to an empirically captured resistance–temperature relationship of device batteries.

The end-of-discharge battery temperature, however, is affected by both device operation and ambient temperature. To meet this challenge, we analyze the thermal behavior of device batteries with a thermal circuit model, capturing the interactions among the battery's discharge current, steady-state temperature, and ambient temperature. Specifically, the steady-state analysis of the thermal model facilitates prediction of battery temperature based on its discharge current and ambient temperature, and its transient-state analysis allows for estimation of ambient temperature based on battery's recent discharge history. Combining these results, EA-SoC learns and updates the thermal characteristics of device battery, and then estimates, in real time, the battery SoC with environment-awareness.

We evaluate EA-SoC with two Nexus 5X smartphones and via 35 experimental case-studies, with [-15, 25]^oC ambient temperature. The results show that EA-SoC reliably captures temperature effect on the remaining usable capacity of batteries, thus achieving accurate SoC estimation even in an environment as cold as -15^oC — phones shut off when EA-SoC concludes they have only ≈3% remaining SoC. On the other hand, such end-of-discharge SoCs provided by the fuel-gauge chips of the phones are averaged at ≈50% for all of the 35 case-studies, indicating a ≈17x improvement by EA-SoC in accurately predicting phones' shutoffs.

This paper makes the following main contributions.

- Empirically capturing the battery's resistance–temperature relationship.
- Characterization of interactions among battery temperature, current, and environment.
- Design of EA-SoC, an environment-aware battery SoC estimation service for mobile devices.
- Evaluation of EA-SoC with 2 Nexus 5X smartphones, showing EA-SoC reports ≈3% end-of-discharge battery SoC even in a -15^oC environment, while that reported by the phones' built-in fuel-gauge chips could be over 90%.

The paper is organized as follows. The background and motivation are presented in Secs. 2 and 3, respectively. Secs. 4–6 detail the design, implementation, and evaluation of EA-SoC, respectively. The related literature is discussed in Sec. 7, and the paper concludes in Sec. 8.

2 BATTERY STATE-OF-CHARGE

Here we introduce the necessary background on the estimation of battery SoC.

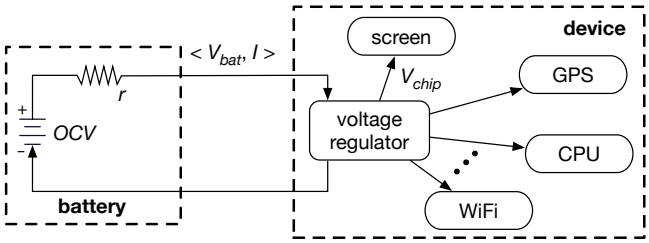

Figure 2: Circuit model of mobile devices: battery provides voltage $V_{bat} = OCV - I \cdot r_{bat}$ to device chips, which has to be higher than a pre-defined level required by the voltage regulator; otherwise, the device will shut off.

2.1 Circuit Model of Mobile Devices

Fig. 2 illustrates the power architecture of mobile devices with a circuit model, consisting of the battery, the individual hardware components of the device, and a voltage regulator connecting them. The device battery is represented as a series connection of an ideal voltage source and its internal resistance r [7, 36]. The ideal voltage source provides a voltage that is commonly referred to as the battery's *open circuit voltage* (OCV), defined as the voltage between its terminals when no loads/charger is connected. This way, the battery supplies a voltage of

$$V_{bat} = OCV - I \cdot r - V_P(I,t) \simeq OCV - I \cdot r \tag{1}$$

to the voltage regulator, where I is the discharge current, t is time, and V_P is a polarization voltage which represents voltage transient over time (t) when it supplies current (I). Note that polarization voltage does not affect ohmic resistance and instantaneous voltage drop in the mobile application. Also, high-rate measurement in a mobile device can capture instantaneous voltage drop by limiting the influence of voltage transient. This allows for simplifing battery equivalent circuit model without the loss of voltage estimation accuracy. The voltage regulator then converts V_{bat} to a required level to power various device modules, such as screen, CPU, etc.

The voltage regulator, however, needs an input voltage (i.e., V_{bat} in Fig. 2) no less than a pre-defined level $V_{shutoff}$; otherwise, it will be unable to provide the required voltage to the device, and thus the device will shut off. According to Eq. (1), a mobile device will shut off when its battery OCV decreases to $V_{shutoff} + I \cdot r$, which is commonly referred to as the *end-of-discharge OCV*, i.e., OCV_{end}.

2.2 Estimation of Battery SoC

SoC quantifies the remaining capacity of a battery, defined as the ratio of battery's remaining usable capacity to its full charge capacity, i.e.,

$$SoC = \frac{C_{remain}}{C_{full}} \times 100\%. \tag{2}$$

Commodity mobile devices estimate their battery SoCs mainly based on the OCV–DoD relationship of their batteries[2]. This is

[2]DoD (depth-of-discharge) describes the battery capacity that has been discharged as a percentage of its maximum capacity. Also, many SoC estimation methods have been proposed in the literature [14, 19, 20]. Here we mainly focus on their basic principles. A complete and detailed example on estimating the battery SoC for mobile devices can be found in [34].

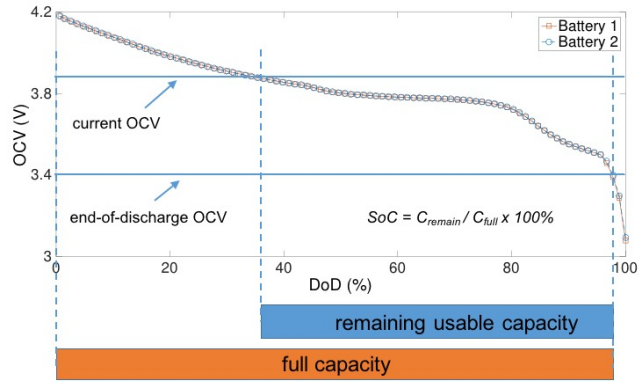

Figure 3: OCV–DoD relationship of batteries: facilitates the estimation of battery SoC based on its OCV.

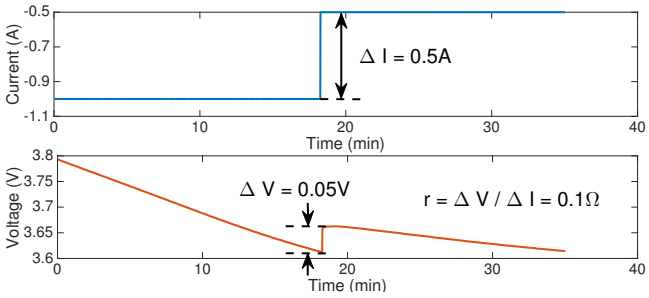

Figure 4: Resistance estimation: estimating a battery's resistance based on the voltage response when switching currents between two stable levels, i.e., $r = \Delta V/\Delta I$.

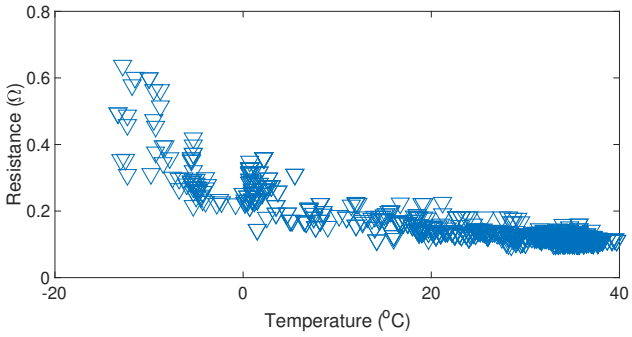

Figure 5: Battery resistance increases with reduced temperature.

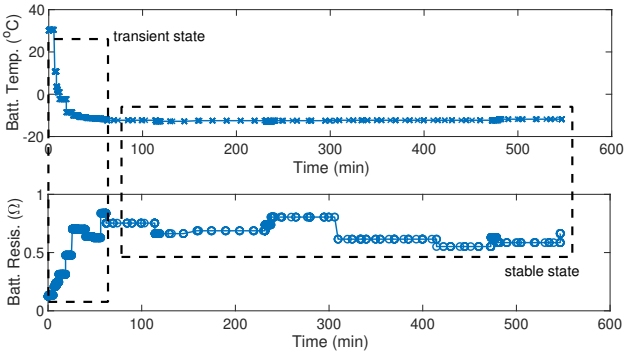

Figure 6: Evolution of battery temperature and resistance after putting into a -12^oC environment.

because Lithium-ion batteries, the most widely used batteries for mobile devices, demonstrate a monotonic relationship between their OCVs and DoDs as shown in Fig. 3. This relationship is tested to be stable for batteries of the same chemistry and does not vary much with manufacturer (e.g., < 5mV variances in OCV with given DoD [1, 18]). We use $d = \mathbb{D}(v)$ to refer to the mapping from battery OCV v to DoD d in the rest of the paper, and will elaborate on how to obtain the OCV–DoD relationship in Fig. 3 in Sec. 5.

Based on this OCV–DoD relationship, mobile device estimates its battery SoC by predicting its end-of-discharge OCV according to

$$OCV_{end} = V_{shutoff} + I_{end} \cdot r_{end}, \tag{3}$$

and then estimating the battery SoC as

$$SoC(t) = \frac{\mathbb{D}(OCV_{end}) - \mathbb{D}(OCV(t))}{\mathbb{D}(OCV_{end})} \times 100\%. \tag{4}$$

Combination of Eqs. (1), (3), and (4) reveals the battery resistance r (both current value and the one at the time at end-of-discharge) is needed to estimate battery OCV. Battery resistance is measured on mobile devices based on the principle of $r = dV/dI$ [26, 34], as illustrated in Fig. 4 with a battery of the Galaxy S3 phone. Switching the discharge current from 1A to 0.5A, the battery voltage recovers instantly from 3.61V to 3.66V, and then reduces gradually again due to continuous discharge. This way, a current change of $|1 - 0.5| =$ 0.5A causes the battery a voltage response of $|3.66 - 3.61| = 0.05$V, indicating a $0.05V/0.5A = 0.1\Omega$ battery resistance according to Ohm's law. However, the two stable current levels (i.e., 1A and $0.5A$ in the above example) are needed to obtain a reliable dI, which are not always available on mobile devices due to their dynamic usage patterns, degrading both the availability and accuracy of real-time resistance.

Moreover, the battery's internal resistance depends strongly on the temperature, complicating its estimation further. To shed more light on this, we log the battery resistance of a Nexus 5X smartphone after putting it in a freezer and until it shuts off. These experiments are repeated 3 times and a total number of 1,263 pairs of battery resistance and temperature are collected, as plotted in Fig. 13: the battery resistance increases dramatically when its temperature drops below 5^oC.

3 UNEXPECTED DEVICE SHUTOFFS IN COLD ENVIRONMENTS

Knowing the basics of batteries and the estimation of their SoC, we next examine why the mobile devices tend to prematurely shut off in cold environments.

Cold temperature slows down the chemical reactions inside the batteries, impeding the batteries to produce the same current and

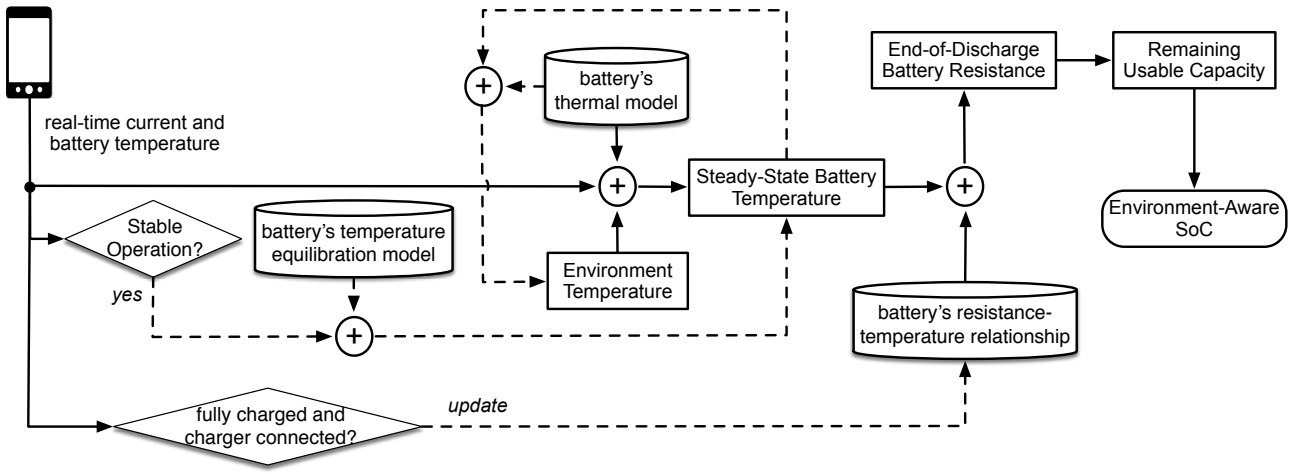

Figure 7: Control flow of EA-SoC: estimating SoC with the awareness of battery's resistance-temperature relationship and by predicting battery's steady-state temperature in real time; such battery characteristics are learned and updated online.

deliver the same capacity as with warmer temperature. This chemical degradation is observed physically as the increase of battery's internal resistance [15, 25, 32], as empirically validated in Fig. 5. Also, such an increase of battery resistance in cold environments occurs gradually. Fig. 6 plots the resistance and temperature of a Nexus 5X phone's battery after putting an idle Nexus 5X phone into a -12^oC environment: (i) the battery temperature reduces gradually to -11.8^oC, and during the same process, (ii) the battery resistance gradually increases to about 0.66Ω. This gradually changing battery information, albeit intuitive, makes the estimation of end-of-discharge battery condition (i.e., Eq. (3)) non-trivial. Let us consider the scenario in which a mobile user is moving from a warm to a cold environment. The fuel-gauge chip of the mobile device will estimate the end-of-discharge condition of the device battery based on its current information, i.e., a resistance measured in a warm environment r_{warm} [34]. Such an estimation, however, is clearly inaccurate because the battery resistance will increase when it is moved to the cold environment, denoted as r_{cold} and $r_{cold} > r_{warm}$. Thus, the device's fuel-gauge chip will underestimate r_{end} in Eq. (3), leading to under-estimation of OCV_{end}. This will, in turn, cause over-estimation of battery SoC according to Eq. (4), thus causing unexpected device shutoffs.

4 ENVIRONMENT-AWARE ESTIMATION OF BATTERY SOC

To mitigate the unexpected shutoffs of mobile devices in cold environments, we design a novel method called EA-SoC to estimate the battery SoC for mobile devices with the awareness of environment temperature.

4.1 EA-SoC Overview

EA-SoC estimates the battery SoC by (i) predicting the end-of-discharge battery temperature, (ii) estimating the end-of-discharge battery resistance based on the thus-predicted temperature, and then (iii) estimating battery SoC based on Eqs. (3) and (4). Fig. 7 provides the flow chart of EA-SoC.

4.2 Predicting the End-of-Discharge Battery Temperature

EA-SoC predicts the end-of-discharge battery temperature by exploiting the interplays between battery temperature and that of the ambient environment. Note that same as with phone's built-in fuel-gauge chips, EA-SoC assumes the recent discharge current of the battery will be kept stable until shutoff [34].

• **Battery's Thermal Model.** Battery temperature T_{bat} is jointly determined by device operation and ambient environment T_{amb}, as shown in Fig. 8 with a *thermal circuit model*. According to Fourier's law, a thermal circuit is analogous to an electric circuit where voltage represents temperature (T_{bat}), current source represents heat generation (P_{bat}), and thermal resistance and capacitance (R_{th}, C_{th}) describes how battery dissipates heat. Since heat conserves, heat generation from the battery must equate to the heat dissipation through thermal capacitance and resistance:

$$C_{th} \cdot \frac{dT_{bat}(t)}{dt} + \frac{T_{bat}(t) - T_{amb}}{R_{th}} = P_{bat}, \tag{5}$$

where the left-hand side is heat dissipation and the right-hand side is heat generation from the battery. Eq. (5) can be further divided into two cases based on $dT_{bat}(t)/dt$: the battery will be in a stable thermal state when $dT_{bat}(t)/dt = 0$, and in a transient thermal state otherwise. Fig. 6 highlights the two-state thermal behavior of batteries. EA-SoC estimates, and update in real time, the (to-be-converged) stable-state battery temperature based on recent battery information, and use it as the battery temperature at the end-of-discharge to estimate the battery SoC.

• **Estimating Battery Temperature via Stable-State Analysis.** Eq. (5) facilitates the identification of battery's steady-state temperature, i.e., the equilibrated battery temperature when $\frac{dT_{bat}(t)}{dt} =$

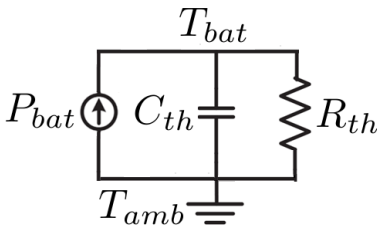

Figure 8: Battery's thermal circuit model: thermal behavior of battery is characterized as thermal resistance (R_th) and capacitance (C_th).

Figure 9: Experimentally validate the relationship among I, T_{bat} and T_{amb}.

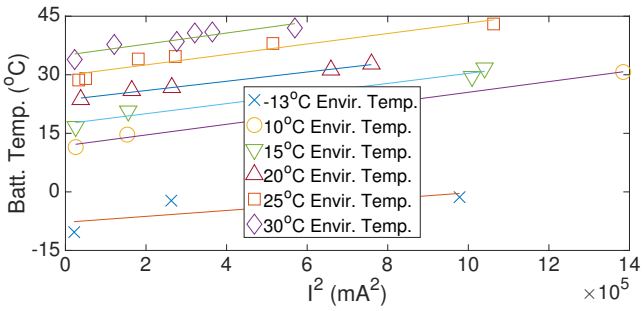

Figure 10: Interactions among battery current, battery temperature, and ambient temperature: linearity between T_{bat} and I^2 is observed, and T_{amb} contributes to T_{bat} as an offset.

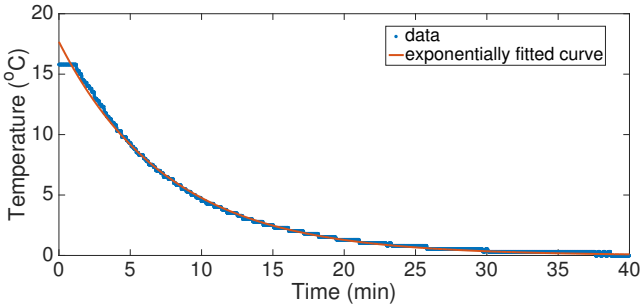

Figure 11: Exponential equilibrating process of battery temperature: battery temperature equilibrates according to the transient temperature model, i.e., $T_{bat}(t) = a_2 \cdot e^{b_2 \cdot t} + c_2$ ($t > 0$).

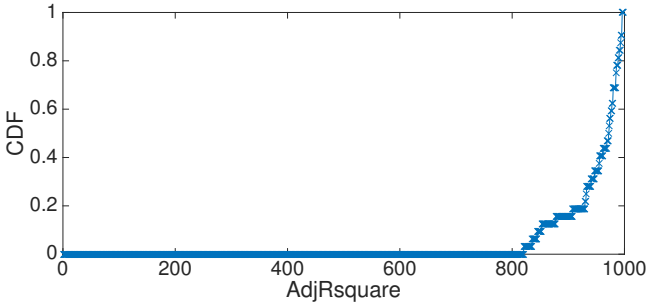

Figure 12: Goodness-of-fit on the exponential equilibrating process based on 34 empirically collected traces: close-to-1 *AdjRsquare* shows promising fitting goodness.

0. Specifically, given stable device operation and ambient environment, battery's steady-state temperature T_{bat} can be calculated as

$$\frac{dT_{bat}(t)}{dt} = 0 \quad \Leftrightarrow \quad \frac{T_{bat}(t) - T_{amb}}{R_{th}} = P_{bat}$$
$$\Leftrightarrow \quad T_{bat} = T_{amb} + R_{th} \cdot P_{\text{bat}}. \tag{6}$$

We can see that (i) T_{bat} is linear to battery's heat dissipation P_{bat}, and (ii) the ambient temperature T_{amb} contributes to T_{bat} as an offset.

Battery's heat generation P_{bat} can be modeled by the Joule's law, and according to Eq. (11), we know

$$P_{bat} = I^2 \cdot r_{bat}$$
$$= I^2 \cdot (a_1 \cdot e^{b_1 \cdot T_{bat}} + c_1 \cdot e^{d_1 \cdot T_{bat}}). \tag{7}$$

Substituting Eq. (7) into Eq. (6), we get

$$T_{bat} = T_{amb} + R_{th} \cdot I^2 \cdot (a_1 \cdot e^{b_1 \cdot T_{bat}} + c_1 \cdot e^{d_1 \cdot T_{bat}}), \tag{8}$$

which can be used to estimate the stable-state battery temperature based on that of the ambient environment.

Next, we empirically validate these observations with a Nexus 5X smartphone. Specifically, we use an Android app called `BatteryDrainer` to regulate the phone operation and thus achieving a (relatively) stable phone operation but with a controllable intensity. The phone, with the thus-regulated operation, is then put in a thermal chamber to achieve controllable ambient temperature, as shown in Fig. 9. We conducted 27 such experiments with $[-13, 30]^o$C ambient temperature, during which the battery temperature and current are logged at 1Hz. Each experiment lasts at least 1 hour which is observed to be long-enough for battery temperature to equilibrate. Fig. 10 plots the experiment results, showing (i) clear linearity between T_{bat} and I^2 (i.e., the key factor in battery's heat generation) and (ii) T_{amb}'s contribution to T_{bat} as a temperature offset, validating the analytical observations in Eq. (8). Also note that all other parameters in Eq. (8) can be identified on mobile devices in practice: R_{th} and $<a_1, b_1, c_1, d_1,>$ can be identified based on collected training samples, and I can be accessed from the devices' fuel-gauge chips.[3]

• Estimating Battery Temperature via Transient-State Analysis. The ambient temperature T_{amb} is needed to predict T_{bat} based on Eq. (8). The sensing of ambient temperature T_{amb}, however, is not supported by most commodity devices,[4] thus requiring the development of a new ambient temperature estimation method. Fortunately, Eq. (5) also allows the transient-state analysis

[3]Current sensing is now pervasively supported by the fuel-gauge chips of mobile devices, although not so a few years ago [33].

[4]To the best of our knowledge, only a few existing device models support ambient temperature sensing, such as Galaxy S4 and Note 3.

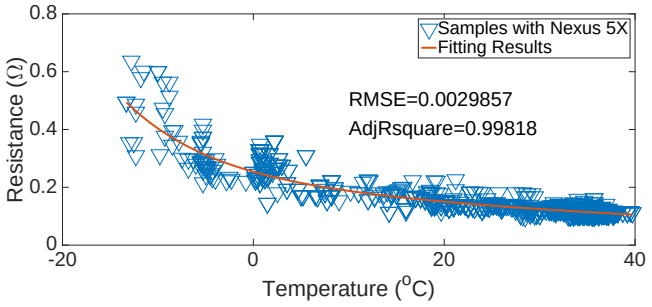

Figure 13: Battery's resistance–temperature relationship: battery resistance $r(T_{bat})$ can be described using a 2-term exponential model with respect to its temperature T_{bat}, i.e., $r(T_{bat}) = a_1 \cdot e^{b_1 \cdot T_{bat}} + c_1 \cdot e^{d_1 \cdot T_{bat}}$.

of battery's thermal behavior, which, when combined with Eq. (8), facilitates the estimation of T_{amb}.

From Eq. (5), the transient-state battery temperature $T_{bat}(t)$ can be described as

$$T_{bat}(t) = (T_0 - (T_{amb} + R_{th} \cdot P_{\text{bat}})) \cdot e^{\frac{-t}{R_{th} \cdot C_{th}}} + T_{amb} + R_{th} \cdot P_{\text{bat}}, \quad (9)$$

where T_0 is battery's initial temperature, and the thermal-time constant, $R_{th} \cdot C_{th}$, represents the time duration required for the battery temperature to stabilize. Note that the second term captures the steady-state temperature while the first term corresponds to the effects of initial temperature, which decays exponentially over time.

Eq. (9) implies the equilibrating process of battery temperature conforms to an exponential process, i.e.,

$$T_{bat}(t) = a_2 \cdot e^{b_2 \cdot t} + c_2, \quad (10)$$

for certain $<a_2, b_2, c_2>$. As a validation, Fig. 11 plots the results when fitting an empirically collected temperature equilibrating process according to Eq. (10), observing an excellent match. Fig. 12 plots the CDF of the goodness-of-fit (in terms of *AdjRsquare*) when exponentially fitting 34 such temperature equilibrating processes, validating the soundness of the exponential model as a close-to-1 *AdjRsquare* indicates promising fitting goodness.

Such an exponential equilibrating process allows EA-SoC to predict the steady-state battery temperature based on its recent temperature traces, if the device has operated stably for a certain amount of time. EA-SoC determines the stable device operation based on its recent current. Specifically, EA-SoC smoothes the recent (e.g., 10 minutes) current trace via moving average, and then applies linear fitting on the smoothened current trace, concluding a stable device operation if the resultant slop factor is small, e.g., ≤ 0.1. In case of stable device operation, EA-SoC trains the exponential model in Eq. (10) based on the recent 10-minute battery temperature trace, i.e., identifying $<a_2, b_2, c_2>$, and using it to predict the steady-state battery temperature, i.e., when $dT_{bat}/dt < 1^oC/5min$. The thus-estimated steady-state battery temperature is then used to estimate the ambient temperature according to Eq. (8). We will experimentally explore the required duration of stable device operation, e.g., 10 minutes in the above explanations, in Sec. 6.

• **Estimating Ambient Temperature.** Now, we have identified two approaches to predict the battery temperature, combination of which forms a feedback loop to estimate the ambient temperature, as shown in Fig. 7: estimates the end-of-discharge battery temperature and the ambient temperature by exploiting battery's transient-state behavior when the device has been operate stably recently, and use the thus-estimated ambient temperature to predict the end-of-discharge battery temperature otherwise.

4.3 Estimating the End-of-Discharge Battery Resistance

EA-SoC then estimates the end-of-discharge battery resistance based on the above predicted end-of-discharge battery temperature. As shown in Fig. 5, batteries' resistance increases with the decrease of temperature, reducing their usable capacity. This explains why commodity mobile devices operate reasonably well in warmer environments (i.e., with relatively stable resistance), but frequently suffer from unexpected shutoffs in a cold environment (i.e., due to increased resistance). Moreover, these empirically-collected samples reveal a 2-term exponential relationship between battery resistance r_{bat} and temperature T_{bat}, i.e.,

$$r_{bat}(T_{bat}) = a_1 \cdot e^{b_1 \cdot T_{bat}} + c_1 \cdot e^{d_1 \cdot T_{bat}}. \quad (11)$$

Fig. 13 plots the regression results when applying such 2-term exponential fit onto the collected samples in Fig. 5, achieving a goodness-of-fit of $RMSE<0.03$ and $AdjRsquare>0.998$.

Inspired by such a resistance–temperature relationship, EA-SoC identifies $<a_1, b_1, c_1, d_1>$ in Eq. (11) based on empirically collected samples of $<r_{bat}, T_{bat}>$, and then estimates the end-of-discharge battery resistance based on the previously predicted the end-of-discharge battery temperature. Four pairs of different $<r_{bat}, T_{bat}>$ are needed to determine $<a_1, b_1, c_1, d_1>$. To enhance reliability and reduce fluctuation, EA-SoC determines $<a_1, b_1, c_1, d_1>$ based on the most recent n ($n \geq 4$) different pairs of $<r, T_{bat}>$ — calculating $<a_1, b_1, c_1, d_1>$ based on each of C_n^4 possible combinations of logged samples, and describing the resistance–temperature relationship with the averaged $<a_1, b_1, c_1, d_1>$. Also, EA-SoC only updates $<a_1, b_1, c_1, d_1>$ when the device is fully charged and the charger is kept connected, which (i) offers reliable conditions to estimate battery resistance [16] and (ii) does not incur any additional overhead in battery energy consumption due to the connected charger and thus the existence of external power supply.

Note that we implicitly assume a uniform temperature distribution across the battery, i.e., describing battery temperature with a single value T_{bat}. This assumption is reasonable as most mobile devices use single-cell batteries which are of much smaller form factors than large multi-cell battery packs, e.g., those for EVs, although Lithium-ion batteries are known to have complex thermal behaviors due to their non-uniform temperature distributions and non-linear chemical reactions. Such a simplification is also widely used in practice — to the best of our knowledge, all commodity mobile devices use a single thermal sensor to monitor their battery temperature, and thus represent their battery temperature with a single temperature reading.

Algorithm 1 Pseudocode of EA-SoC.

```
1: initializing <a1, b1, c1, d1> and T_amb;
2: while true do
3:    estimate steady-state battery temperature according to Eq. (8)
      with I and T_amb;
4:    estimate end-of-discharge battery resistance according to
      Eq. (11)
5:    estimate end-of-discharge OCV according to Eq. (3);
6:    estimate remaining usable capacity and thus SoC;
7:    estimate SoC via Coulomb counting;
8:    if stable operation for the past 10 minutes then
9:       predict steady-state battery temperature T_bat according to
         Eq. (10);
10:      update T_amb according to Eq. (8);
11:   end if
12:   if phone is fully charged and the charger is still connected
      then
13:      update <a1, b1, c1, d1>;
14:   end if
15:   time = time + 1;
16: end while
```

4.4 Estimating Battery SoC with Temperature Awareness

At last, EA-SoC estimates the end-of-discharge battery OCV based on the predicted r_{end} according to Eq. (3), and then further estimates the battery SoC based on Eqs. (1) and (4).

4.5 EA-SoC Summary

Alg. 1 summarizes EA-SoC in the form of pseudocode. EA-SoC estimates the steady-state battery temperature based on the discharge current and ambient temperature with current and ambient temperature (i.e., Eq. (8) and line 3), which is then used to predict the end-of-discharge battery resistance according to Eq. (11) (line 4). This way, the end-of-discharge OCV can be calculated as in Eq. (3) (line 5). EA-SoC then estimates battery SoC based on the OCV–DoD relationship as in Eq. (4) (line 6). EA-SoC updates the knowledge of (i) ambient temperature T_{amb} when the device has been working reliably for, e.g., 10 minutes (line 9-10), and (ii) the resistance-temperature model after the device has been fully charged and the charger is still connected (line 13).

5 IMPLEMENTATION

Given below are a few details of EA-SoC's implementation.

5.1 Logging of Battery Information

EA-SoC monitors and logs real-time information on battery current and temperature, based on which the device's SoC is estimated with environment-awareness. This battery information can be obtained from the devices' fuel-gauge chips, e.g., the system files of `current_now` and `temp` under directory `/sys/class/power_supply/battery/` for Nexus 5X and Nexus 6P. The real-time logging of such information, however, incurs energy consumption to the device. So, EA-SoC is desired to collect battery information at a low frequency while ensuring sufficient SoC estimation accuracy. Note that the fuel-gauge chips of mobile devices easily support up to 1Hz (or higher, depending on specific device models) sampling rates of battery information, which, for example, can be adjusted on the Android platform by configuring the fuel-gauge driver at `drivers/power/qpnp-fg.c`.

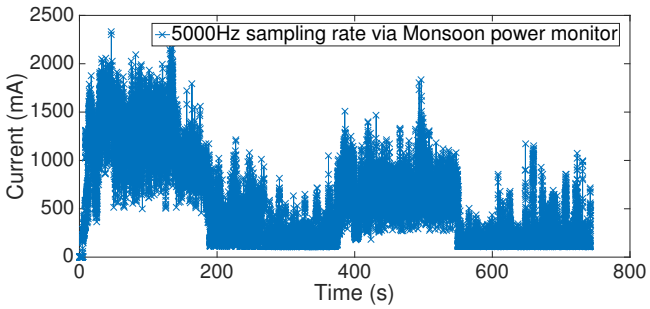

Figure 14: Current trace of a Galaxy S5 phone with 5,000Hz sampling rate: based on which the impact of current sampling rate on fuel-gauging accuracy is investigated.

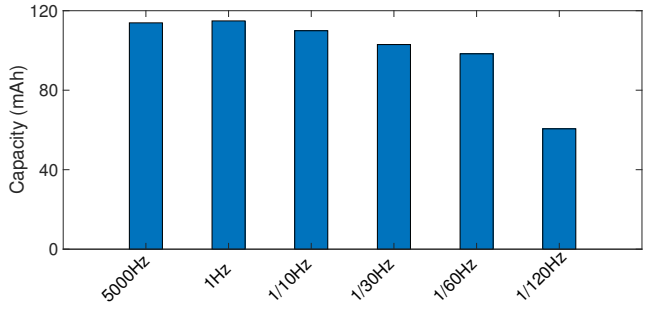

Figure 15: Effects of current sampling rate: 1/10Hz sampling rate can achieve over 99% fuel-gauging accuracy.

We empirically identify such proper sampling rates on battery temperature and current. First, we examine the frequency for battery temperature to change based on the 34 temperature equilibrating processes as used in Fig. 12, which are originally collected at 1Hz sampling frequency. This way, we find that the battery temperature changes every 8.9s, on average, based on a total of 17,212 samples. Second, the current information is needed to quantify the device's energy consumption. To identify the necessary current sampling rate for accurate fuel gauging, we collected a 12-minute current trace from a Galaxy S5 phone with the Monsoon power monitor running at 5kHz, as shown in Fig. 14, during which 114mAh capacity is discharged. Using this trace, we calculate the total energy consumption when emulating different current sampling rates of 1Hz, 1/10Hz, 1/30Hz, and 1/60Hz, achieving the discharged capacity of 115mAh, 113mAh, 109mAh, and 98mAh, respectively — a 1/10Hz sampling rate is able to achieve over 99% fuel-gauge accuracy, as shown in Fig. 15. Combining the above empirical observations, EA-SoC monitors and logs battery temperature and current once every 8s.

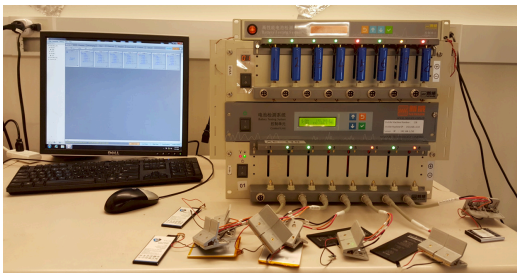

Figure 16: Using the battery testing system to identify battery's OCV–SoC relationship

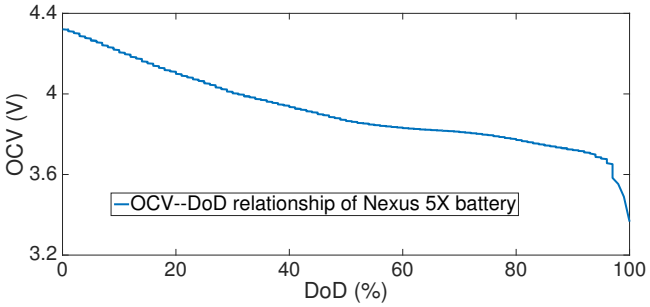

Figure 17: Empirically identified OCV–SoC relationship of Nexus 5X battery

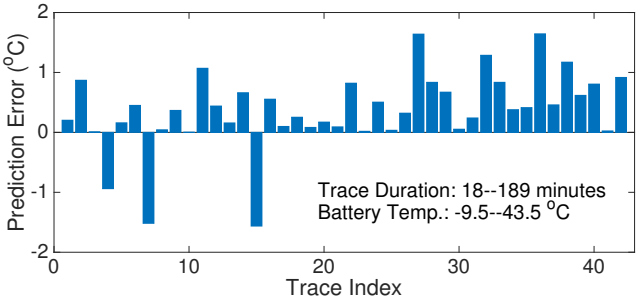

Figure 18: Predicting future battery temperature based on its exponential equilibrating process: <2°C prediction error when training with 18-minute temperature trace.

5.2 Identifying the OCV–DoD Relationship

EA-SoC needs the OCV–DoD relationship of device battery to estimate its DoD, which is collected via offline training. Given a specific model of mobile device, e.g., Nexus 5X, we use the battery tester as in Fig. 16 to discharge its battery with 200mA current and log the process at 1Hz, collecting traces on the relationship between the battery terminal voltage and its DoD. We then perform resistance compensation on the thus-collected traces based on Eq. (1) to derive its OCV–DoD table. The small current of 200mA is to reduce the $I \cdot r_{bat}$ voltage and thus improve the accuracy of the derived OCD–DoD table. Fig. 17 shows the thus-collected OCV–DoD relationship of a Nexus 5X battery. The OCV–DoD relationship shown in Fig. 3 is collected similarly.

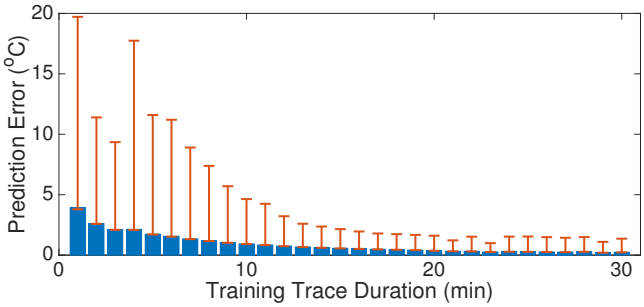

Figure 19: Needed training duration: a 10-minute training trace is able to achieve <1°C prediction error.

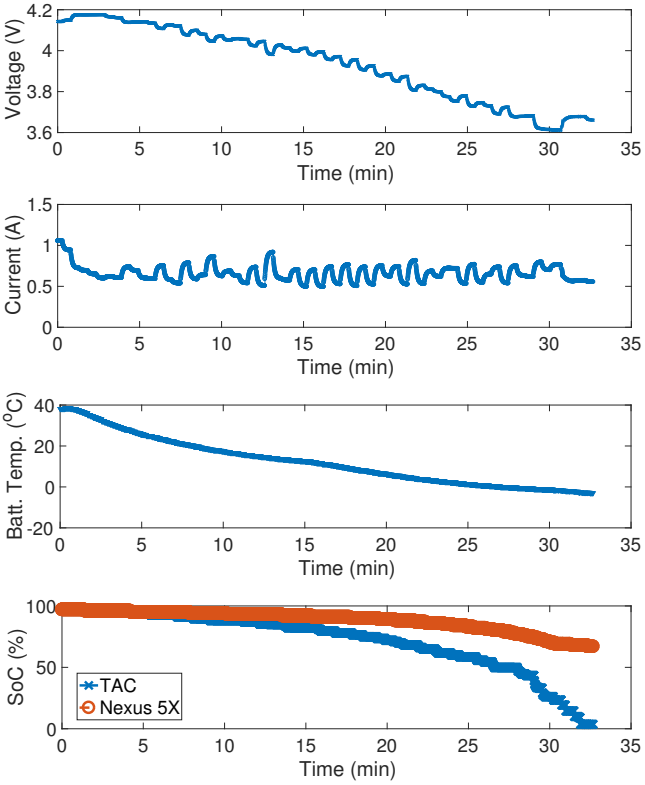

Figure 20: Temperature-compensated SoC estimation: EA-SoC provides more reliable SoC information to users than existing estimations provided on Nexus 5X smartphone.

6 EXPERIMENTS

We have evaluated EA-SoC extensively with two Nexus 5X smartphones.

6.1 Accuracy in Predicting Battery Temperature

We first validate the reliability of predicting battery temperature based on its exponential equilibrating process, i.e., Eq. (10). Specifically, we collected 42 temperature equilibrating processes of a

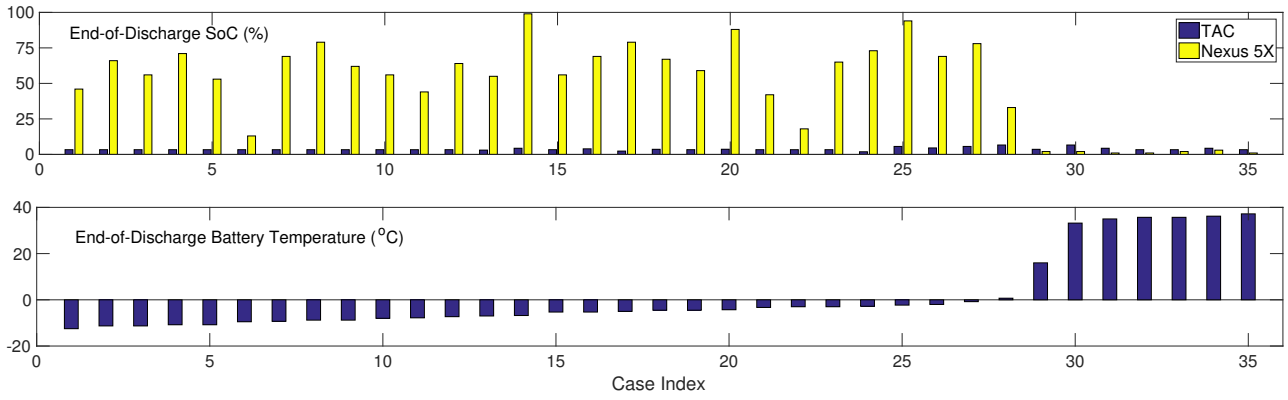

Figure 21: Environment-aware SoC estimation with 35 case-studies: EA-SoC achieves (i) much more reliable SoC estimation in a cold environment, and (ii) comparable results in a warmer environment, compared to the existing SoC estimation on Nexus 5X smartphone.

Nexus 5X phone's battery, while keeping the phone in stable operation conditions. These traces last for $[18, 190]$ minutes and the battery temperature varies in the range of $[-9.5, 43]^oC$. We then use the first x minutes of these traces to train the exponential equilibrating model in Eq. (10), and then use the thus-trained models to predict the battery temperature at the end of their respective traces.

Fig. 18 summarizes the prediction errors when the first 18-minute portion of each trace is used for training, showing within $\pm 2^oC$ errors for all the 42 traces and an average error of 0.366^oC. To further examine how long a stable operation is needed to train a reliable model, Fig. 19 plots the average prediction error for the 42 traces when training with the first x-minute traces, together with their 5- and 95-percentiles[5] — higher prediction accuracy could be achieved by training with longer traces, while a 10-minute training trace is enough to achieve less than 1^oC prediction error.

6.2 Accuracy of SoC Estimation

We next validate EA-SoC's accuracy in estimating battery SoC with 35 case-studies. The thus-estimated environment-aware SoCs are then compared with those provided by the phones, further validating EA-SoC's reliability in predicting phones' shutoffs. Specifically, in each of these case-studies, the phones are used for either Youtubing, or playing an offline video, or kept idle but with screen on, until it shuts off. The experiments start with a $[37, 100]$% phone battery SoC, and are conducted in a $[-15, 28]^oC$ environment. The real-time SoCs estimated by EA-SoC, together with those provided by the phone's fuel-gauge chips, are logged. Note that a closer-to-0 end-of-discharge SoC indicates higher reliability in predicting the phone's shutoffs.

Fig. 20 plots the battery voltage, current, temperature, and estimated SoC during one of such case-studies. Specifically, the fully-charged phone is put into a -13^oC environment, and operates without human interactions until it shuts off, at which time its fuel-gauge chip provides an SoC estimation of about 67% — i.e., the phone shuts off unexpectedly. This case-study finishes with a 3.66V end-of-discharge battery voltage, which is much higher than the usual level, e.g., [3.2, 3.4]V [17], owing to the increased battery resistance at a low temperature. On the other hand, EA-SoC captures the decreased battery temperature in real time, and compensates the SoC estimation accordingly — the phone shuts off when EA-SoC concludes its battery only has a 3.8% SoC, showing EA-SoC's ability to predict the phone's shutoff accurately.

Fig. 21 summarizes the end-of-discharge SoCs collected in all the 35 case-studies, together with, and sorted according to, their end-of-discharge battery temperature. The phones shut off with high and random phone-provided SoCs when their batteries' end-of-discharge temperature is low — they are `high` because the low temperature and thus increased battery resistance, and they are `random` because the phones operate with different currents. By capturing the battery's resistance–temperature dependency, EA-SoC is able to predict the phones' shutoffs much more accurately, achieving a 3% averaged end-of-discharge SoC for the 28 case-studies with end-of-discharge battery temperature lower than 1^oC. Also, EA-SoC performs well in a warmer environment and achieves similar end-of-discharge SoCs as the phones' fuel-gauge chips, as observed in the 29th–35th case-studies.

7 RELATED WORK

Many SoC estimation methods have been proposed in the literature [14, 19, 20], including the OCV-based methods [21, 24], Coulomb counting [23], neural network methods [11], and various Kalman filter-based methods [9, 12, 35]. For example, He *et al.* [18] proposed a model to eliminate the effects of current drift in the current sensor, improving Coulomb counting accuracy. A method to improve re-initialization of Coulomb counting is developed in [29]. A multi-cell battery pack SoC estimation considering cell imbalance is proposed in [37]. Trinh [28] explored ways to validate the SoC estimation accuracy. An empirical study of comparison of various SoC estimation methods can be found in [10].

Of these existing SoC estimation methods, combining the OCV-based method and Coulomb counting to estimate real-time battery SoC is the most widely used for commodity mobile devices,

[5] Only the traces with a duration longer than x minutes are used for validation.

thanks to its simplicity and reasonably good accuracy. Examples of such deployment include TI's `Impedance Track` [34] and Maxim's `MAX17047/17050` fuel-gauge chips [3], to name a few. However, the dependency between battery performance and temperature is still not covered well forcommodity mobile devices, causing them to shut off unexpectedly in a cold environment [6].

To address such deficiency, we have proposed `EA-SoC`, an environment-aware SoC estimation service for mobile devices, achieving accurate SoC estimation even in cold environments. To the best of our knowledge, the closest to `EA-SoC` is [27], which also considers battery temperature in its SoC estimation. The method proposed therein, however, requires various fundamental battery properties such as solid phase diffusion coefficient and electrolyte diffusion coefficient, which are not available on mobile devices due to the limited hardware support.

8 CONCLUSIONS

In this paper, we have designed, implemented, and validated `EA-SoC`, an environment-aware battery SoC estimation service for mobile devices. `EA-SoC` captures the resistance–temperature relationship of device batteries with an empirically established regression model, and estimates battery SoCs based on the thermal interactions among battery's discharge current, steady-state temperature, and ambient temperature. Such interactions are uncovered by a thermal circuit model of the battery and validated experimentally. We have evaluated `EA-SoC` with two Nexus 5X smartphones, achieving ≈3% end-of-discharge SoC even in a -15^{o}C environment and improving reliability in predicting device shutoffs by 17x.

REFERENCES

[1] [n. d.]. Battery Monitoring Basics. https://training.ti.com/sites/default/files/BatteryMonitoringBasics.ppt.

[2] [n. d.]. iPhone 5 Shutting down, Cold Weather or defective battery. https://discussions.apple.com/thread/4742928?tstart=0 .

[3] [n. d.]. MAX17047/MAX17050 ModelGauge m3 Fuel Gauge.

[4] [n. d.]. Nexus 6P goes from 15% to 0% almost straight away. https://productforums.google.com/forum/#!topic/nexus/SeB67voFk38.

[5] [n. d.]. Samsung Galaxy S4 turns off but still has 30% battery life. http://forums.androidcentral.com/samsung-galaxy-s4/303065-samsung-galaxy-s4-turns-off-but-still-has-30-battery-life.html.

[6] [n. d.]. Sub-Zero Weather: Can Your Smartphone Stand The Cold? http://www.pcworld.com/article/249134/sub_zero_weather_can_your_smartphone_stand_the_cold_.html.

[7] 2001. Temperature-dependent battery models for high-power Lithium-Ion batteries. *NREL/CP-540-28716* (2001).

[8] Hoque Mohammad A. and Tarkoma Sasu. 2015. Understanding Smartphone State of Charge Anomaly. In *HotPower'15*.

[9] Dave Andre, Christian Appel, Thomas Soczka-Guth, and Dirk Uwe Sauer. 2013. Advanced mathematical methods of SOC and SOH estimation for Lithium-ion batteries. *Journal of Power Sources* 224 (2013), 20 – 27.

[10] A. Berrueta, I. S. Martin, P. Sanchis, and A. Ursia. 2016. Comparison of State-of-Charge estimation methods for stationary Lithium-ion batteries. In *IECON 2016 - 42nd Annual Conference of the IEEE Industrial Electronics Society*. 2010–2015.

[11] M. Charkhgard and M. Farrokhi. 2010. State-of-charge estimation for lithium-ion batteries using neural networks and EKF. *IEEE Transactions on Industrial Electronics* 57 (2010), 4178–87.

[12] Haifeng Dai, Xuezhe Wei, Zechang Sun, Jiayuan Wang, and Weijun Gu. 2012. Online cell {SOC} estimation of Li-ion battery packs using a dual time-scale Kalman filtering for {EV} applications. *Applied Energy* 95 (2012), 227–237.

[13] O. Erdinc, B. Vural, and M. Uzunoglu. 2009. A dynamic lithium-ion battery model considering the effects of temperature and capacity fading. In *2009 International Conference on Clean Electrical Power*. 383–386. https://doi.org/10.1109/ICCEP.2009.5212025

[14] Thomas C. Greening, Jeffrey G. Koller, Nils E. Mattisson, and P. Jeffrey Ungar. 2015. Estimating state of charge (SoC) and uncertainty from relaxing voltage measurements in a battery.

[15] A. Hande. 2006. Internal battery temperature estimation using series battery resistance measurements during cold temperatures. *Journal of Power Sources* 158, 2 (2006), 1039 – 1046. Special issue including selected papers from the 6th International Conference on Lead-Acid Batteries (LABAT 2005, Varna, Bulgaria) and the 11th Asian Battery Conference (11 ABC, Ho Chi Minh City, Vietnam) together with regular papers.

[16] Liang He, Sunmin Kim, and Kang G. Shin. 2016. ∗-Aware Charging of Lithium-ion Battery Cells. In *ICCPS'16*.

[17] L. He, G. Meng, Y. Gu, C. Liu, J. Sun, T. Zhu, Y. Liu, and K. G. Shin. 2016. Battery-aware mobile data service. *IEEE Transactions on Mobile Computing* PP, 99 (2016), 1–1.

[18] Yao He, XingTao Liu, ChenBin Zhang, and ZongHai Chen. 2013. A new model for State-of-Charge (SOC) estimation for high-power Li-ion batteries. *Applied Energy* 101 (2013), 808 – 814. Sustainable Development of Energy, Water and Environment Systems.

[19] T. Kim, W. Qiao, and L. Qu. 2013. Online SOC and SOH estimation for multicell Lithium-ion batteries based on an adaptive hybrid battery model and sliding-mode observer. In *ECCE'13*.

[20] M. El Lakkis, O. Sename, M. Corno, and D. Bresch Pietri. 2015. Combined battery SOC/SOH estimation using a nonlinear adaptive observer. In *ECC'15*.

[21] S. Lee, J. Kim, J. Lee, and B. Cho. 2008. State-of-charge and capacity estimation of lithium-ion battery using a new open-circuit voltage versus state-of-charge. *Journal of Power Sources* 185 (2008), 1367–73.

[22] A. Millner. 2010. Modeling Lithium Ion battery degradation in electric vehicles. In *2010 IEEE Conference on Innovative Technologies for an Efficient and Reliable Electricity Supply*. 349–356.

[23] KS Ng, CS Moo, YP Chen, and YC Hsieh. 2009. Enhanced coulomb counting method for estimating state-of-charge and state-of-health of lithium-ion batteries. *Applied Energy* 86 (2009), 1506–11.

[24] MA. Roscher and DU. Sauer. 2011. Dynamic electric behavior and open-circuit-voltage modeling of LiFePO4-based lithium ion secondary batteries. *Journal of Power Sources* 196 (2011), 331–6.

[25] Noboru Sato. 2001. Thermal behavior analysis of lithium-ion batteries for electric and hybrid vehicles. *Journal of Power Sources* 99, 1-2 (2001), 70 – 77.

[26] Hans-Georg Schweiger, Soosma Obidi, Oliver Komesker, Andre Raschke, Michael Schiemann, Christian Zehner, Markus Gehnen, Michael Keller, and Peter Birke. 2010. Comparison of several methods for determining the internal resistance of Lithium ion cells. *Sensors* 10 (2010), 5604 – 5625.

[27] Tanvir R. Tanim, Christopher D. Rahn, and Chao-Yang Wang. 2015. State of charge estimation of a lithium ion cell based on a temperature dependent and electrolyte enhanced single particle model. *Energy* 80 (2015), 731–739. https://doi.org/10.1016/j.energy.2014.12.031

[28] Freddy Trinh. 2012. A method for evaluating battery state of charge estimation accuracy. *Master Thesis, Chalmers University of Technology* (2012).

[29] C. Unterrieder, C. Zhang, M. Lunglmayr, R. Priewasser, S. Marsili, and M. Huemer. 2015. Battery state-of-charge estimation using approximate least squares. *Journal of Power Sources* 278 (2015), 274–286.

[30] W.T. Vanderslice and C.J. Scafidi. 1994. Battery heating system using internal battery resistance. https://www.google.com/patents/US5362942 US Patent 5,362,942.

[31] J. Vetter, P. Novák, M.R. Wagner, C. Veit, K.-C. Möller, J.O. Besenhard, M. Winter, M. Wohlfahrt-Mehrens, C. Vogler, and A. Hammouche. 2005. Ageing mechanisms in lithium-ion batteries. *Journal of Power Sources* 147, 1–2 (2005), 269 – 281.

[32] Wladislaw Waag, Stefan Käbitz, and Dirk Uwe Sauer. 2013. Experimental investigation of the lithium-ion battery impedance characteristic at various conditions and aging states and its influence on the application. *Applied Energy* 102 (2013), 885 – 897. Special Issue on Advances in sustainable biofuel production and use - {XIX} International Symposium on Alcohol Fuels - {ISAF}.

[33] Fengyuan Xu, Yunxin Liu, Qun Li, and Yongguang Zhang. 2013. V-edge: Fast Self-constructive Power Modeling of Smartphones Based on Battery Voltage Dynamics. In *NSDI'13*.

[34] Ming Yu, Yevgen Barsukov, and Michael Vega. 2008. Theory and Implementation of Impedance Track Battery Fuel-Gauging Algorithm in bq2750x Family. *Application Report, SLUA450* (2008).

[35] Z. Yu, R. Huai, and L. Xiao. 2015. State-of-Charge Estimation for Lithium-Ion Batteries Using a Kalman Filter Based on Local Linearization. *Energies* 8 (2015), 7854–7873.

[36] Lide Zhang, B. Tiwana, R.P. Dick, Zhiyun Qian, Z.M. Mao, Zhaoguang Wang, and Lei Yang. 2010. Accurate online power estimation and automatic battery behavior based power model generation for smartphones. In *CODES+ISSS'10*.

[37] Liang Zhong, Chenbin Zhang, Yao He, and Zonghai Chen. 2014. A method for the estimation of the battery pack state of charge based on in-pack cells uniformity analysis. *Applied Energy* 113 (2014), 558 – 564.